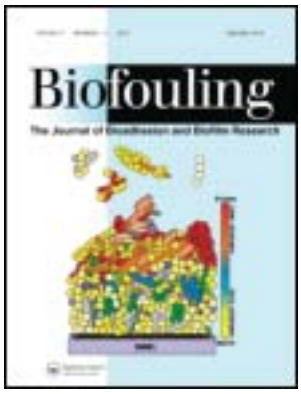

Biofouling: The Journal of Bioadhesion and Biofilm Research

Publication details, including instructions for authors and subscription information:
http://www.tandfonline.com/loi/gbif20

Mini-review: Convection around biofilms

Philip S. Stewart [a]

[a] Center for Biofilm Engineering and Department of Chemical and Biological Engineering, Montana State University – Bozeman, Bozeman, Montana, 59717-3980, USA

Available online: 21 Feb 2012

To cite this article: Philip S. Stewart (2012): Mini-review: Convection around biofilms, Biofouling: The Journal of Bioadhesion and Biofilm Research, 28:2, 187-198

To link to this article: http://dx.doi.org/10.1080/08927014.2012.662641

Biofouling
Vol. 28, No. 2, February 2012, 187–198

Taylor & Francis
Taylor & Francis Group

Mini-review: Convection around biofilms

Philip S. Stewart*

Center for Biofilm Engineering and Department of Chemical and Biological Engineering, Montana State University – Bozeman, Bozeman, Montana 59717-3980, USA

(*Received 2 November 2011; final version received 25 January 2012*)

Water that flows around a biofilm influences the transport of solutes into and out of the biofilm and applies forces to the biofilm that can cause it to deform and detach. Engineering approaches to quantifying and understanding these phenomena are reviewed in the context of biofilm systems. The slow-moving fluid adjacent to the biofilm acts as an insulator for diffusive exchange. External mass transfer resistance is important because it can exacerbate oxygen or nutrient limitation in biofilms, worsen product inhibition, affect quorum sensing, and contribute to the development of tall, fingerlike biofilm clusters. Measurements of fluid motion around biofilms by particle velocimetry and magnetic resonance imaging indicate that water flows around, but not through biofilm cell clusters. Moving fluid applies forces to biofilms resulting in diverse outcomes including viscoelastic deformation, rolling, development of streamers, oscillatory movement, and material failure or detachment. The primary force applied to the biofilm is a shear force in the main direction of fluid flow, but complex hydrodynamics including eddies, vortex streets, turbulent wakes, and turbulent bursts result in additional force components.

Keywords: biofilm; hydrodynamics; mass transfer; Reynolds number; Sherwood number; Peclet number; detachment

Introduction

Microorganisms that attach to a surface interact with their environment through the water that flows over the biofilm. This interaction yields surprisingly complex hydrodynamic and coupled convection-diffusion phenomena. A simple change in the flow velocity can affect the overall rate of substrate consumption in a wastewater treatment biofilm (Horn et al. 2002; Masic et al. 2010), alter the pattern of gene expression in a research system or metabolic activity (Simões et al. 2007, 2008; Singer et al. 2011), perturb the ecology of a mixed species biofilm (Rochex et al. 2008; Besemer et al. 2009), lead to the detachment and dissemination of an infectious biofilm (Fux et al. 2004), or modulate the efficacy of an anti-biofilm treatment agent (Simões et al. 2005; Eberl and Sudarsan 2008). There are two important ways that fluid flow influences microbial biofilm development and activity that are examined in this review: the transport of dissolved solutes into and out of the biofilm, and the application of forces to the biofilm that cause it to move and detach.

This article is not intended to be a comprehensive review of the literature. The author's hope is that this discussion will illustrate phenomena and describe general relationships in a way that is accessible and useful to a broad and interdisciplinary audience. The review focuses on the elementary engineering science behind biofilm-hydrodynamic interactions. The reader may also wish to consult some prior reviews (Characklis et al. 1990; Purevdorj-Gage and Stoodley 2004; de Beer and Stoodley 2006).

Convection influences solute exchange between the bulk fluid and biofilm

Solute transport between flowing water and biofilm is not easy to visualize experimentally. Perhaps the best way to capture this phenomenon in action is by using microelectrode technology to directly measure concentration profiles. Consider for example the oxygen concentration profile published by Kühl and Jørgensen (1992) and reproduced in Figure 1. This profile was measured on a trickling filter biofilm that was grown on a stone in a sewage treatment plant. The biofilm covered rock was brought back to the laboratory and aerated medium was circulated over it. The bulk fluid velocity was approximately 5 cm s^{-1}. The bulk fluid concentration of oxygen was approximately 270 μM. The oxygen concentration decreased to approximately 150 μM at the interface between the flowing fluid and the biofilm. This drop in oxygen concentration outside the biofilm was not due to consumption of oxygen in the fluid phase; all of the respiratory activity was localized inside the biofilm. Instead, the relatively slow

*Email: phil_s@biofilm.montana.edu

ISSN 0892-7014 print/ISSN 1029-2454 online

http://dx.doi.org/10.1080/08927014.2012.662641
http://www.tandfonline.com

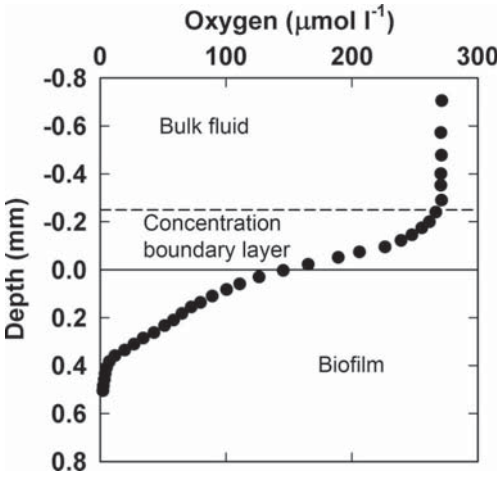

Figure 1. External mass transfer resistance made evident in the change in concentration of oxygen outside a trickling filter biofilm. The bulk fluid concentration of oxygen was ~270 μM. The oxygen concentration decreased to approximately 150 μM at the interface between the flowing fluid and the biofilm. Oxygen diffused across the fluid zone, sometimes termed a concentration boundary layer, to reach the biofilm. [Redrawn with permission from Kühl and Jørgensen 1992.]

moving fluid adjacent to the biofilm posed a barrier to the transport of oxygen from the bulk fluid to the biofilm surface. Oxygen had to diffuse across this fluid film, sometimes termed a concentration boundary layer or mass transfer boundary layer, to reach the biofilm. Inside the biofilm, oxygen was completely consumed within about 500 μm. In this example, about half the overall change in oxygen concentration in the system occurred outside the biofilm and could therefore be attributed to external mass transfer resistance. This term is used to distinguish mass transport limitation that occurs external to the biofilm from diffusion limitation that occurs internally (Stewart 2003).

Diffusion boundary layers above biofilms have been measured in a wide variety of research and real-world systems including the leaves of a freshwater macrophyte (Nishihara and Ackerman 2007), a diatom canopy (Roberts et al. 2007), and biomineralizing stromatolites (Bissett et al. 2008). See Figure 2 for a recent visualization of oxygen concentration around a biofilm in two dimensions (Staal et al. 2011).

One way to quantify external mass transfer resistance is through the physical dimension of the concentration boundary layer. In the example shown in Figure 1, this layer was approximately 250 μm thick. Another way to quantify external mass transfer is with a mass transfer coefficient. This parameter, denoted here by k_L, is defined by:

$$J = k_L(C_o - C_s),$$

where C_o is the bulk fluid concentration of a solute, C_s is the concentration of the solute at the biofilm–bulk fluid interface, and J is the flux of solute into the biofilm. The mass transfer coefficient has units of velocity and it should be noted that it is a solute-specific parameter. The concentration boundary layer thickness, here denoted by L_L, and the mass transfer coefficient are related by:

$$k_L = D_{aq}/L_L$$

where D_{aq} is the aqueous diffusion coefficient of the solute of interest. A third way to quantify external mass transfer is with a Sherwood number:

$$Sh = dk_L/D_{aq},$$

which is simply a dimensionless version of the mass transfer coefficient. The variable d is a characteristic dimension of the system such as the diameter of a tube or the depth of the fluid flowing over the top of the biofilm.

There are many articles that report measurements of external mass transfer coefficients in biofilm systems (Siegrist and Gujer 1987; Zhang and Bishop 1994; Zhu and Chen 2001; Wäsche et al. 2002). Data from a few of these are plotted in Figure 3 as Sherwood number *vs* Reynolds number, *Re* (La Motta 1976; Horn and Hempel 1995; Bishop et al. 1997; Rasmussen and Lewandowski 1998). For the purposes of this discussion, this plot can be thought of as dimensionless mass transfer coefficient *vs* dimensionless flow velocity. A few conclusions can be drawn from this figure. The first is that the relationship between *Sh* and *Re* depends on the geometry of the system. A tube and flat plate, for example, behave differently. Second, there is a general trend of increasing mass transfer coefficient with increasing flow velocity, as would be intuited. Many theoretical and empirical relationships have been derived or described to relate *Sh* and *Re* in various systems (eg Gantzer et al. 1988; Debus et al. 1994; Li and Chen 1994; Christiansen et al. 1995; Zhu and Chen 2001). These formulae take the form of

$$Sh \approx Re^n$$

where the exponent, n, typically ranges from 1/3 to 1. For the aggregate data plotted in Figure 3, the relationship between the two numbers is approximated by

$$Sh = 0.6Re^{0.69} \text{ for } 10^2 \leq Re \leq 10^4$$

The third conclusion, and it is a cautionary one, is that there is considerable variability in the value of the

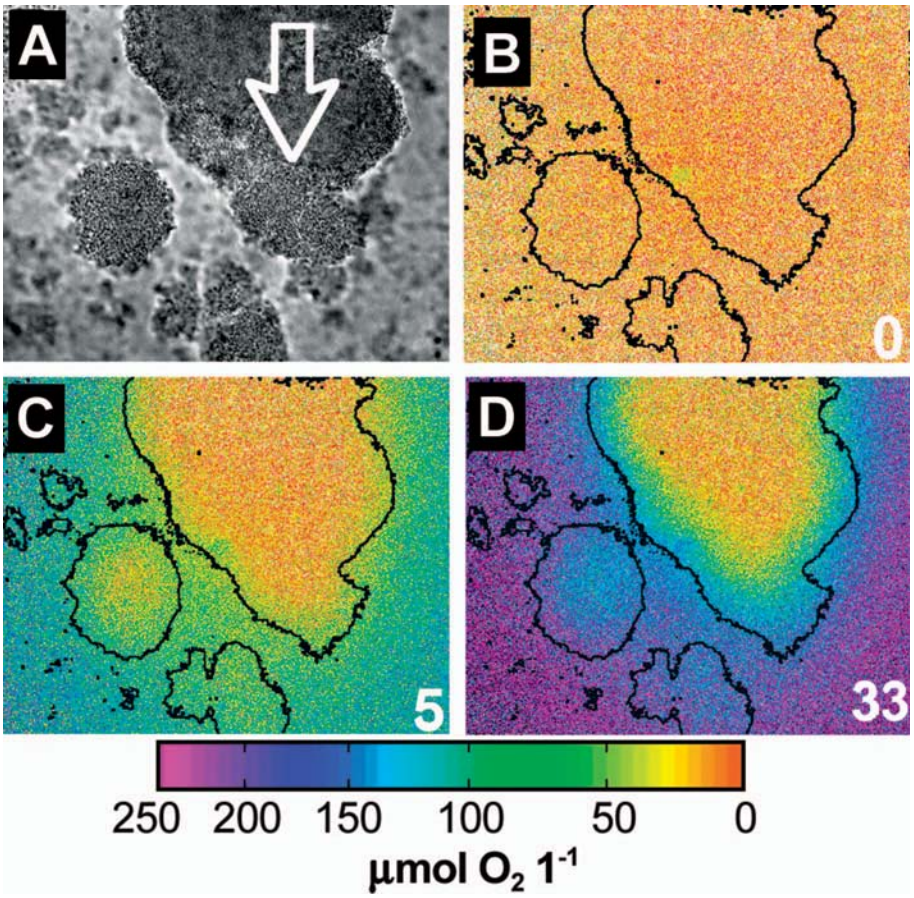

Figure 2. Oxygen concentration at the base of a biofilm imaged at various flow rates. The oxygen concentration beneath a biofilm cluster, imaged in transmitted light mode in panel A, was measured using optode technology which quantifies the oxygen concentration at all points on the substratum. Flow was in the direction of the arrow. Under stagnant conditions (B), oxygen was depleted over the entire field. At a bulk flow velocity of 5 m h^{-1} (C), gradients in oxygen concentration were evident both internal and external to the biofilm cluster. At a higher flow rate of 33 m h^{-1}, external gradients were mostly eliminated. [Reprinted with permission from Staal et al. 2011.]

external mass transfer coefficient, even within a given experimental data set. Because of the heterogeneous architecture of many biofilms, and also the complex hydrodynamics, the local mass transfer coefficient can differ between two adjacent spots in the same biofilm (de Beer et al. 1994b; Yang and Lewandowksi 1995; Rasmussen and Lewandowski 1998). The measurements collected in Figure 3, when analyzed in terms of the concentration boundary layer thickness, span two orders of magnitude from 11 to 1100 μm.

In most biofilm systems, Sherwood numbers larger than 1000 would be expected to correspond to negligible external mass transfer resistance.

The most significant consequence of external mass transfer limitation is to exacerbate transport limitation into or out of the biofilm. External mass transfer resistance decreases the concentration of metabolic substrates seen by the biofilm and increases the concentrations of metabolic products within the biofilm. It also decreases the overall flux of substrates and products in or out of the biofilm. The flux of oxygen into a respiring biofilm is throttled by the presence of the slow-moving fluid film outside, which acts like an insulator. The egress of a metabolic product out of the biofilm can likewise be slowed by external mass transfer resistance. The pH change that occurs inside a biofilm when a metabolic reaction either consumes (eg denitrification) or produces (eg sugar fermentation to acids) protons is thus magnified by external mass transfer resistance. Modeling studies predict a role for hydrodynamics in the phenomenon of quorum sensing, which also involves the local accumulation of a metabolic product (Horswill et al. 2007; Kirisits et al. 2007; Vaughan et al. 2010).

A striking consequence of external mass transfer resistance is the development of towers or fingered growth (Figure 4). These structures arise by growth of the biofilm in a concentration gradient of substrate.

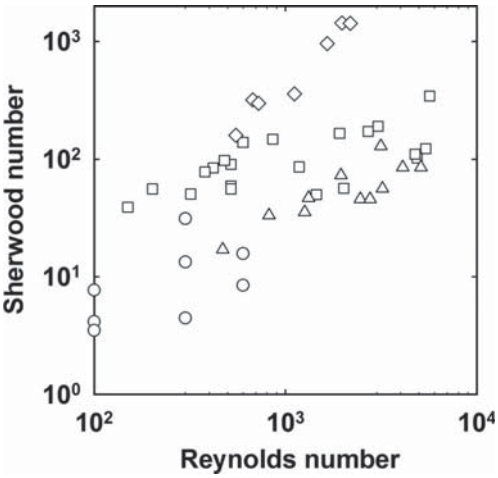

Figure 3. Sherwood number (dimensionless mass transfer coefficient) *vs* Reynolds number. The data are from: annular reactor, La Motta (1976) (△); circular tube, Horn and Hempel (1995) (◇); submerged flat plate, Bishop et al. (1997) (□); submerged flat plate, Rasmussen and Lewandowski (1998) (○).

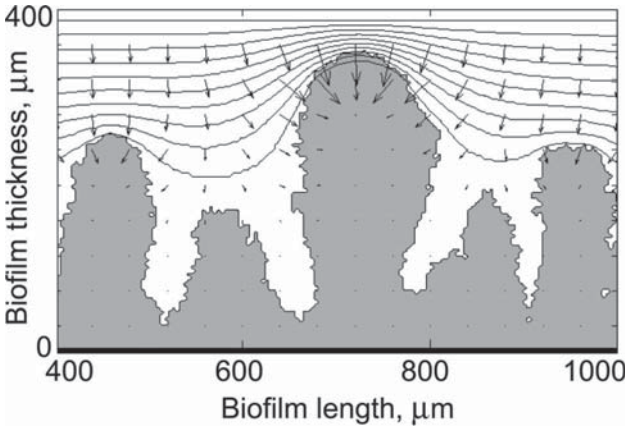

Figure 4. Tower-like biofilm structures (gray) develop due to mass transfer limitation in a computer model simulation [reprinted with permission from Picioreanu et al. (1998)]. Lines show contours of equal substrate concentration and arrows indicate the direction and magnitude of the local substrate flux. This view shows a cross section with the attachment substratum along the bottom and the source of substrate along the top. As the tops of biofilm cell clusters access more substrate, they grow faster than other parts of the cluster and thereby amplify height differences to eventually produce tall clusters separated by channels.

This effect is most clearly evinced in theoretical models (Picioreanu et al. 1998; Hermanowicz 1999; Dockery and Klapper 2001; van Loosdrecht et al. 2002). Initial small differences in the height of biofilm structures are amplified as the tips of these structures access the highest concentration of substrate, experience more rapid microbial growth, and so expand faster than other parts of the biofilm. This phenomenon may contribute to the heterogeneous architecture of some biofilms; it is expected to be most influential under conditions of slow flow and pronounced external mass transfer resistance. Other complex interactions between biofilm structure, hydrodynamics, and microbial growth have been explored (Picioreanu et al. 2000; Roy et al. 2002; Ohl et al. 2004; Yu et al. 2004; Picioreanu et al. 2009).

Stagnation is an important special case in which there is a breakdown in external mass transfer. Under no-flow conditions, diffusion is the sole solute transport process and the fluid adjacent to the biofilm will become depleted in the limiting metabolic substrate and enriched in metabolic waste products.

Evidence for fluid flow around, but not inside, biofilm cell clusters

The complexity of convection in biofilms is normally hidden from view because the flow of clean water is invisible. Experimenters have been able to visualize and make measurements of fluid flow by particle tracking velocimetry and magnetic resonance imaging. By imaging the movement of neutrally buoyant particles at different heights above a biofilm, velocity profiles have been constructed (de Beer et al. 1994a; Stoodley et al. 1994, 1997; Bishop et al. 1997). In every case, the fluid velocity diminished and approached zero close to the biofilm surface. When the biofilm consisted of cell clusters separated by water channels, flow in the channels could be detected by the motion of microbeads (Figure 5).

NMR-based techniques have enabled non-invasive, three-dimensional mapping of water velocities in tubular (Manz et al. 2003; Seymour et al. 2004a; Gjersing et al. 2005; Hornemann et al. 2009; Wagner et al. 2010) and other biofilm systems (Lewandowski et al. 1992, 1993; Seymour et al. 2004b). Though the spatial resolution of magnetic resonance microscopy is less than that of light microscopy, magnetic resonance imaging measurements also support an interpretation of water flow around, but not through, biofilm cell clusters (Figure 6).

Another way to approach the question of convection within biofilm cell clusters is by analysis of hydraulic permeability. According to Darcy's law, the fluid velocity in a porous medium is given by

$$v = \frac{k}{\mu}\nabla P$$

where k denotes hydraulic permeability, μ is fluid viscosity, and ∇P is the pressure gradient. This relationship will be used to estimate the magnitude of

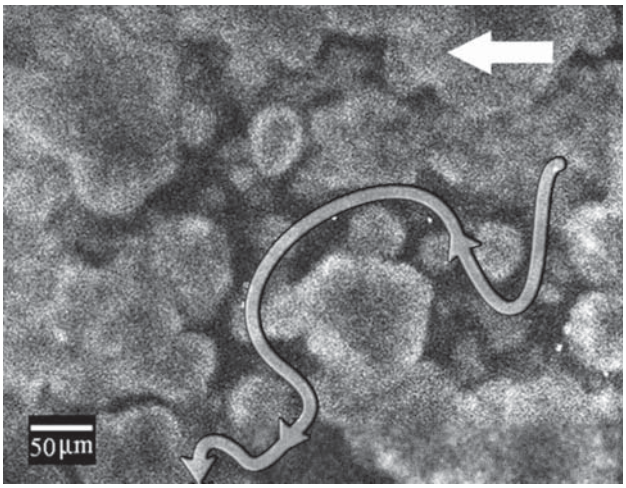

Figure 5. Experimental demonstration of fluid flow near bacterial biofilms by particle tracking [reprinted with permission from Stoodley et al. (1994)]. The white block arrow indicates the direction of bulk flow. The transparent arrowed path indicates the circuitous route taken by fluorescent microbeads through the water channels (dark) of the biofilm (light).

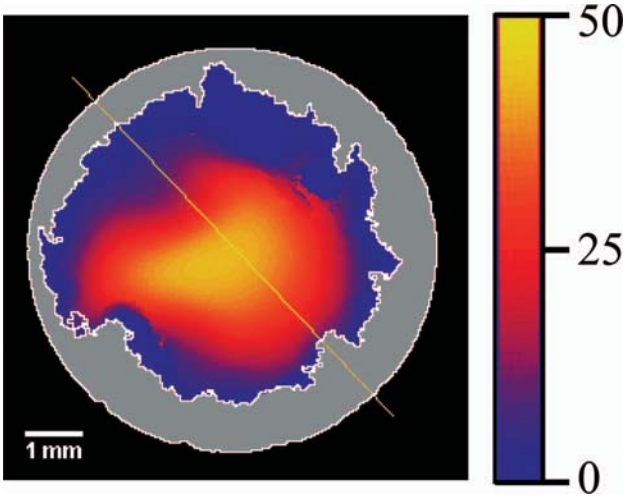

Figure 6. Experimental demonstration of fluid flow near bacterial biofilm (gray) in a circular tube by magnetic resonance imaging [reprinted with permission from Manz et al. (2003)]. The Reynolds number was 84. The colorscale gives the local velocity in mm s^{-1}.

the flow induced inside a biofilm by a pressure gradient. The viscosity, μ, can be taken as the viscosity of water for the purposes of this order-of-magnitude calculation; a value of 10^{-3} kg m^{-1} s^{-1} is used.

Some relevant experimental measurements of hydraulic permeabilities in microbial aggregates or hydrogels are summarized in Table 1. Biofilms are understood to be mixtures of bacterial cells embedded

Table 1. Hydraulic permeabilities in hydrogels and microbial aggregates.

Material	(m^2) k	Source
Agar gel	4×10^{-15}	McDonogh et al. (1994)
Activated sludge filter cake	2×10^{-16}	McDonogh et al. (1994)
Bacterial filter cake	5×10^{-17}	McDonogh et al. (1994)
Immobilized *E. coli*	4×10^{-16}	Fowler and Robertson (1991)
Agarose gel, 2%	4×10^{-16}	Johnson and Deen (1996)
Agarose gel, 7%	2×10^{-17}	Johnson and Deen (1996)

in a hydrogel matrix made up of polysaccharides, proteins, and nucleic acids. Theories of flow, in for example a periodic array of spheres (Sangani and Acrivos 1982; as calculated by Libicki et al. 1988), tend to overestimate the permeabilities indicated by measurements reported in Table 1. This suggests that the predominant resistance to flow in a microbial aggregate is posed by extracellular matrix material. An upper bound on the hydraulic permeability of a biofilm cell cluster is 1×10^{-15} m^2.

The magnitude of the pressure gradient was calculated for two situations representative of biofilm environments. For turbulent flow in a pipe, an experimentally measured pressure gradient was of the order of magnitude of 4×10^3 N m^{-3} (Picologlou et al. 1980). For a fluid film falling down a vertical surface, the pressure gradient is $\sim 10 \times 10^3$ N m^{-3}.

Combining these three parameter or variable estimates in the Darcy equation yields a fluid velocity, inside a biofilm cell cluster, of 10^{-8} m s^{-1} or 0.01 μm s^{-1}. This nearly imperceptible speed is consistent with the experimental measurements discussed above.

Does water flow inside biofilm cell clusters? Probably not, unless the cluster is fractured. Because of the heterogeneous structure of biofilms and the fact that they block flow, biofilms divert the bulk flow and create velocity components in directions other than the primary flow direction. This is evident in the microbead experiment shown in Figure 5, and these secondary flows have been imaged and quantified by magnetic resonance microscopy (Seymour et al. 2004a; Gjersing et al. 2005; Hornemann et al. 2009). In a model capillary system under laminar flow, secondary flows as large as 20% of the axial flow velocity have been reported (Hornemann et al. 2009).

Advective solute transport inside biofilm cell clusters is negligible

Here, the question of whether convection contributes to solute transport within the cell clusters of a biofilm

is addressed. This is not an easy question to answer because even though flow inside a cell cluster may be very slow, the transport of a solute by bulk fluid flow (advection) is generally much more rapid than is transport by diffusion. A slow flow may be sufficient to contribute to, or even dominate, transport of a substrate or product. To deal with this issue properly requires a comparison of the rates of advective and diffusive transport. This comparison is captured in a dimensionless parameter known as the Peclet number. An order of magnitude estimation of the Peclet number inside a biofilm follows.

Inside a biofilm, within a microbial cell cluster, the processes of solute reaction, diffusion, and convection can be analyzed with a differential material balance of the form

$$\frac{\partial u}{\partial \tau} = \nabla^2 u - Pe\nabla u - \varphi^2 g(u)$$

where u is a dimensionless substrate concentration and t a dimensionless time. The dimensionless parameter φ is a Thiele modulus that compares the relative rates of reaction and diffusion. The dimensionless parameter Pe is a Peclet number that compares the relative rates of convection and diffusion. When $\mathrm{Pe} \gg 1$, convective transport is more important than diffusive transport and when $\mathrm{Pe} \ll 1$, diffusive transport is more important that convective transport. The Peclet number is therefore a convenient means of assessing the significance of convective flow on solute transport. It is defined by

$$Pe = \frac{vL}{D_e}$$

where v is a characteristic fluid velocity, D_e is the effective diffusivity, and L is a characteristic length scale. An upper bound on fluid velocity was just calculated as 10^{-8} m s^{-1}.

Effective diffusivities in biofilms have been discussed in a previous article (Stewart 1998). For the purpose of this paper, oxygen will be used as a representative solute. The mean relative effective diffusivity of oxygen in biofilms was found to be ~ 0.5 (Stewart 1998). Combining this with the known value of the diffusion coefficient of oxygen in water at 25°C, which is 2.0×10^{-9} m^2 s^{-1} (Han and Bartels 1996), D_e is estimated to be 1×10^{-9} m^2 s^{-1}. A typical characteristic length of a microbial cluster in the direction of flow is ~ 100 μm. The Peclet number is found to be 10^{-3}. The small value of Pe indicates that convection inside the biofilm is insignificant as an oxygen transport process. For reference, Nir and Pismen (1977) calculated that, in order to obtain a 50% increase in the effectiveness factor (ie the observed reaction rate), the Peclet number would have to be at least 10. This result suggests that, while convection may occur in water channels permeating biofilms, within actual cell clusters diffusion is the predominant transport process.

This theoretical conclusion is supported by experimental studies that visualize the transport of fluorescent molecules (de Beer et al. 1994a, 1997; Rani et al. 2005; Stewart et al. 2009). For example, a bolus of fluorescein injected into a void within a biofilm, forms a plume that elongates in the direction of flow. The same microinjection within a cell cluster retains its spherical symmetry. de Beer et al. (1994a) concluded: 'Liquid can flow through the voids, whereas, in the cell clusters, liquid is stagnant. Consequently, in the voids mass transport may take place by both convection and diffusion, whereas, in the cell clusters, only diffusion can occur.' Using time-lapse confocal scanning laser microscopy, investigators have been able to watch the penetration of fluorescent molecules into biofilm cell clusters under continuous flow conditions (Rani et al. 2005; Stewart et al. 2009). These visualizations reveal identical penetration of an antibiotic on the upstream and downstream edges of a cell cluster, indicating no perceptible influence of convective transport inside the cluster (Figure 7).

Fluid flow influences biofilm movement, deformation, and detachment

Fluid flow around the biofilm applies forces to the biofilm that can cause it to deform or detach (Figure 8). The fluid–structure interactions between moving water and microbial biofilm lead to a surprising variety of behaviors. These include viscoelastic deformation explored from experimental (Stoodley et al. 1999, 2001a, 2002; Dunsmore et al. 2002; Brindle et al. 2011) and theoretical approaches (Towler et al. 2006; Alpkvist and Klapper 2007; Vo et al. 2010; Vo and Heys 2011), rolling (Rupp et al. 2005), rippling (Purevdorj and Stoodley 2004; Stoodley et al. 2005), development of streamers (Stoodley et al. 1998; Rusconi et al. 2010, 2011), oscillatory movement (Stoodley et al. 1998; Taherzadeh et al. 2010), and material failure or detachment (Stoodley et al. 2001b, 2002; Alpkvist and Klapper 2007; Graba et al. 2010; Wagner et al. 2010).

The predominant force acting on the biofilm is a shear force, exerted in the direction of flow. This force is referenced to a corresponding substratum area to yield the wall shear stress, the force acting in the direction of flow per unit area of substratum. The force can be accessed through the fluid mechanician's tool of the friction factor, denoted by f. To best illuminate the relationship between force applied to the biofilm and

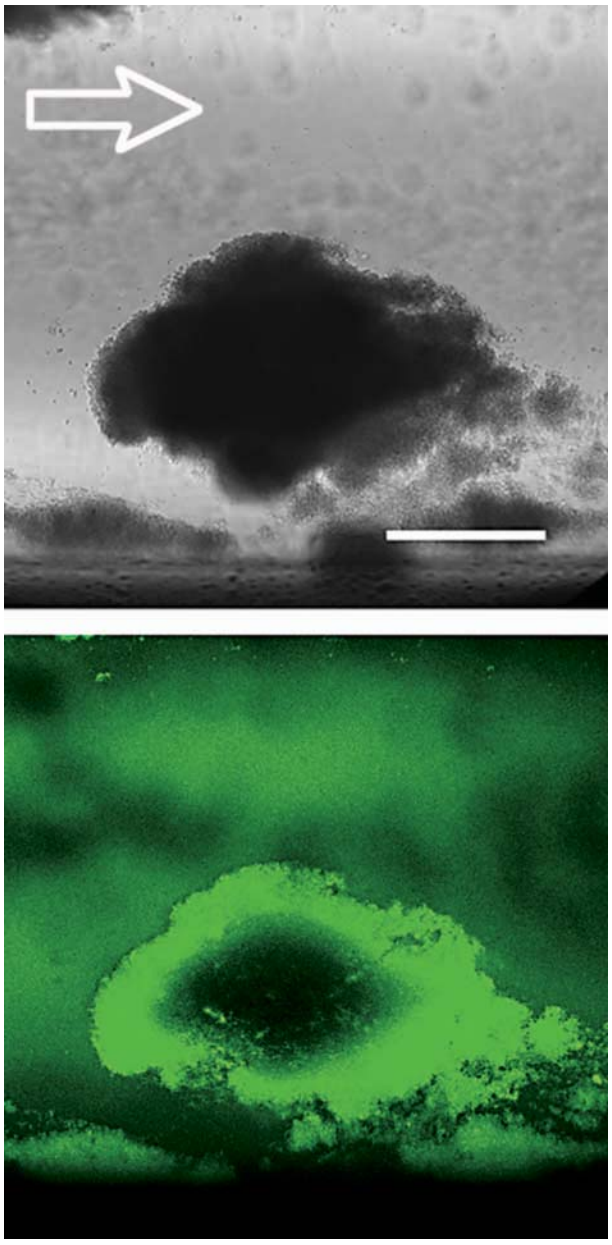

Figure 7. Symmetric transport of a fluorophore-tagged antibiotic into a biofilm cell cluster under continuous flow conditions [previously unpublished image collected as per Stewart et al. (2009)]. A transmission image shows a *Staphylococcus epidermidis* biofilm cluster as a dark area (top). At a time point 1 min after the introduction of fluorescent daptomycin (green/grey in print) into the flow cell, the drug has penetrated a similar distance at the upstream and downstream edges of the cluster (bottom). Flow was from left to right at an average clean-tube velocity of 2 cm s^{-1}. Over a period of 1 min, bulk convective flow at this speed would carry the antibiotic 120 cm or approximately 3000 times the dimension of the biofilm cluster. Scale bar = 200 μm.

fluid velocity, a conventional friction factor plot has been replotted as a dimensionless wall shear stress (Γ) *vs* Reynolds number (Figure 9). This analysis assumes zero fluid velocity (no slip) at the biofilm or substratum surface. The transition from laminar to turbulent flow evident in Figure 9 represents a qualitative change from a macroscopically well-ordered flow pattern (laminar) to a flow that includes small but continuous fluctuations in the velocity components of the overall flow (turbulent). What this plot makes obvious is the strong dependence of shear stress on fluid velocity. As with the Sherwood number, the shear stress displays a power law dependence on Reynolds number:

$$\Gamma \approx Re^{n}$$

In laminar flow, theoretical derivations demonstrate that shear stress is directly proportional to *Re*; the exponent $n = 1$. In transition or turbulent flow, the dependence is stronger with n expected to be between 7/4 and 2. One experimental biofouling investigation reported an exponent value of 1.84 (Stoodley et al. 1998). The take home message from this analysis is that flowing fluid exerts a force on the biofilm that increases sharply with the flow velocity.

When the surface over which fluid flows is rough, the frictional resistance is increased (dashed lines in Figure 9). Biofilm formation can contribute to surface roughness and so increase wall shear stress and pressure drop (Picologlou et al. 1980; Schultz and Swain 1999).

When examined at the microscale, varied and complex hydrodynamic behaviors are anticipated around biofilm structures. Even under laminar flow conditions, recirculating eddies can form, both on the upstream and downstream faces of a biofilm protuberance. As the flow velocity increases, the size of the eddies on the downstream side is expected to increase. Possible flows include paired eddies circulating in the plane of the substratum, or a vertical circulation in a plane perpendicular to the substratum. The convergence of the flow over the top of a biofilm cluster with an upward recirculating flow has the potential to pinch and elongate the biomass into a streamer on the downstream side. As with other obstacles to flow, a biofilm cluster can shed vortices in an unsteady flow termed a Kármán vortex street. A biofilm streamer exposed to these two parallel rows of translating, staggered vortices would be expected to oscillate from side to side, as has been experimentally observed (Stoodley et al. 1998) and computationally confirmed (Taherzadeh et al. 2010). At higher velocities, the laminar flow impinging on the upstream edge of a biofilm cluster can break up into a turbulent wake on the downstream side. In turbulent flows, microscale packets of energetic fluid termed turbulent bursts may penetrate the laminar sublayer and impinge transiently

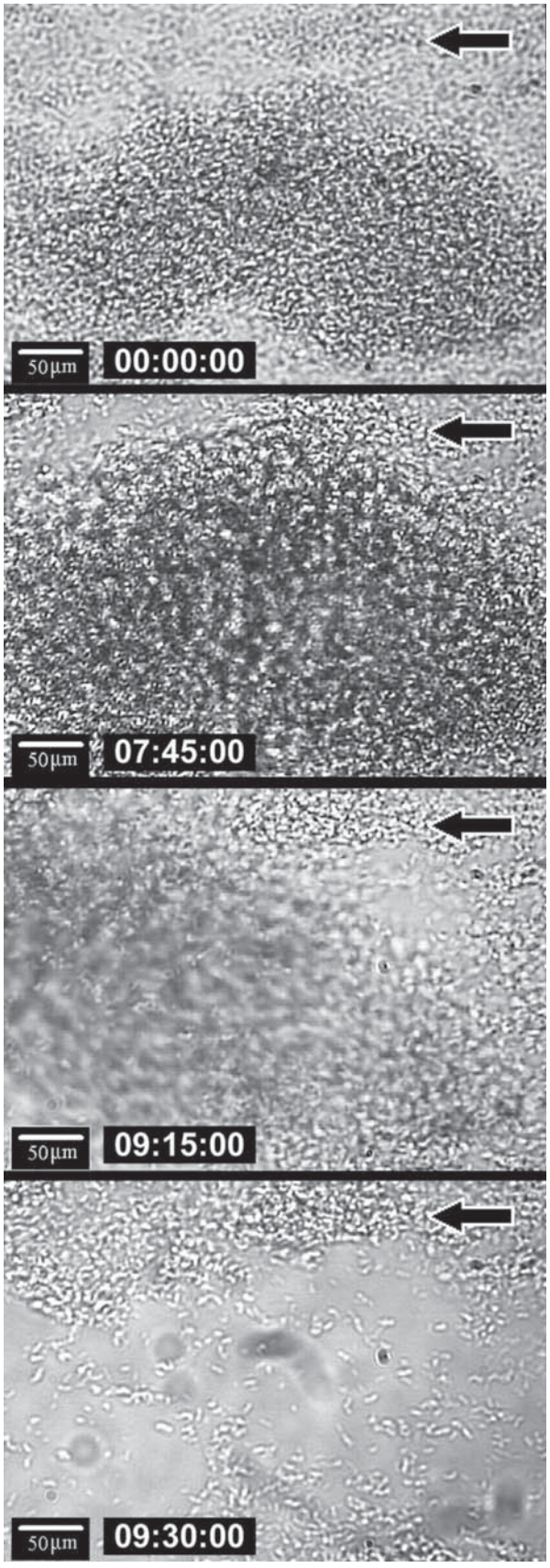

Figure 8. Hydrodynamic deformation and detachment of a biofilm cell cluster. Flow was from right to left as indicated by the arrow. The view is looking down on the biofilm from the fluid. As the cluster grows and becomes taller, it is deformed in the direction of flow. The cluster is eventually sheared from the surface, leaving behind a few attached cells. [Unpublished data courtesy of Paul Stoodley collected in the experimental system described in Stoodley et al. (2001b)]. A video of this sequence can be viewed in the supplementary online material.

on the biofilm. The complexity of flows described above mean that there can be force components applied to a biofilm in directions other than the shear force acting in the direction of bulk fluid flow. These forces contribute to deformation, movement, mixing, and removal of biomass.

Computational fluid dynamic models allow for insight into the complex hydrodynamics and fluid structure interactions that are possible even in simple geometries (Picioreanu et al. 2009; Salek et al. 2011; Teodósio et al. 2011; Yang et al. 2011). For more insight into hydrodynamics the reader is encouraged to seek out the beautiful Album of Fluid Motion (van Dyke 1982) and a computational counterpart at www.featflow.de/album/index.html.

One consequence of biofilm formation is to increase the drag force on a surface over which water moves, such as a boat hull or pipe. In a conduit, the result is an increased pressure drop. The y-axis of

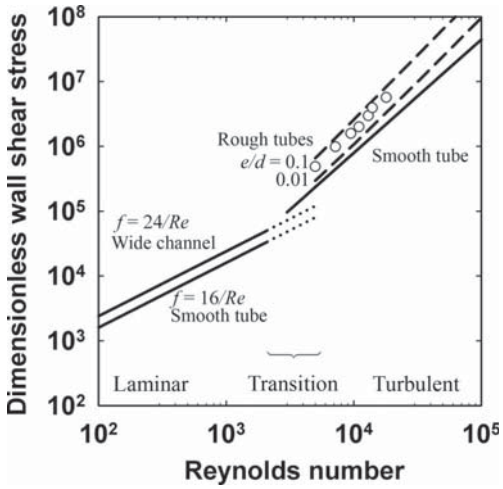

Figure 9. Dimensionless wall shear stress *vs* Reynolds number. The shear stress was calculated as fRe^2. Smooth tube turbulent flow was calculated from the Blasius equation (Characklis et al. 1990). Rough tube turbulent flow results (dashed lines) were calculated from the Colebrook equation for two different relative roughness (e/d) values (Characklis et al. 1990). The open circles are data from Picologlou et al. (1980) for a 300 μm thick biofilm grown in a circular tube.

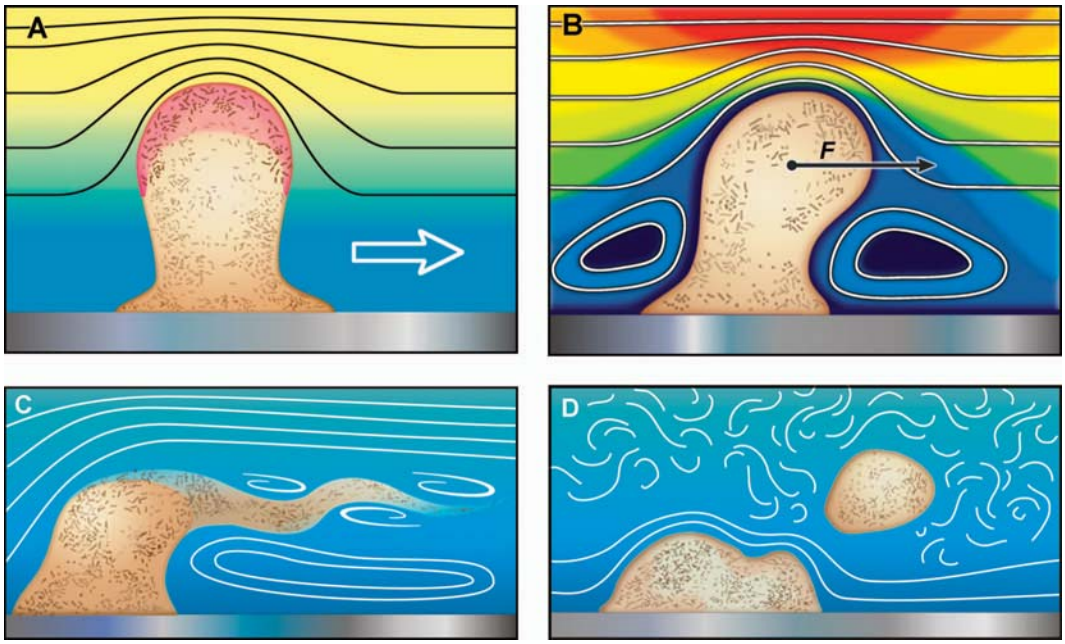

Figure 10. Effects of fluid flow on microbial biofilm. The four panels illustrate different phenomena, and correspond to increasing fluid velocity from A to D. The direction of fluid flow (block arrow) is from left to right. Solid lines are pathlines, the trajectory of an individual fluid particle. (A) Especially in slow flows, the fluid can pose resistance to diffusive transport of solutes (metabolic substrate, eg oxygen, indicated in yellow) exacerbating limitations within the biofilm. Rapid cell growth (pink) is restricted to the regions of the biofilm with access to substrate. These regions expand preferentially, leading to fingering of biofilm structures. (B) Fluid moves around biofilm cell clusters, but not through them. Hotter colors (red) indicate high fluid velocity, colder colors (blue) indicate slower fluid velocity. Moving fluid applies a force to the biofilm (arrow). Complex secondary flows, such as eddies, can occur even under laminar flow conditions. (C) Fluid flow can induce deformation and movement of the biofilm, such as the formation of oscillating streamers on the downstream edge of a cell cluster. (D) When the force applied by the fluid exceeds the cohesive strength, the biofilm can fail leading to a detachment event. Turbulent flow produces bursts that penetrate to the immediate environs of the biofilm and result in brief, but intense force excursions. The dimension of biofilm structures like those cartooned here typically range from tens of microns to millimeters.

Figure 9 could equivalently be labeled dimensionless pressure drop. Biofouling increases the pressure drop by occluding the conduit, roughening the surface, and by dissipating energy through the motion of the biofilm.

The extent of biofilm accumulation in a given system is a complex integration of the nutrient availability, hydrodynamics, and antimicrobial pressure. Consider the trade-off involved in increasing the flow velocity over a biofilm between enhanced mass transfer and enhanced detachment. In a relatively slow flow regime, increasing flow velocity is expected to allow for a thicker biofilm by enhancing mass transfer of substrate into the biofilm. As the flow rate is further increased, detachment may dominate and so result in a thinner biofilm. Just such behavior has been observed experimentally (Zhang et al. 2011). The efficacy of biocides, antibiotics, or anti-biofilm agents is intertwined with the system hydrodynamics (Simões et al. 2005; Cogan et al. 2008; Eberl and Sudarsan 2008; Davison et al. 2010). In particular, the efficacy of biofilm removal agents depends on the action of fluid shear to work in concert with weakening effects of the agent itself to detach biomass (Simões et al. 2005; Lee et al. 2008; Davison et al. 2010; Brindle et al. 2011).

Summary

Convection is an important process in the fluid around a microbial biofilm. The following summary points are emphasized and diagrammed schematically in Figure 10: (1) slow moving fluid near the biofilm poses a barrier to diffusive transport of solutes into and out of the biofilm; (2) fluid moves around, but not through, biofilm cell clusters; (3) hydrodynamics can be complex around the heterogeneous structures of a biofilm; (4) moving fluid applies forces to the biofilm; (5) convection can induce deformation of the biofilm and movement by stretching, rolling, and rippling; and (6) fluid forces can cause biofilm detachment.

Acknowledgement

Artwork was prepared with the expert technical assistance of Peg Dirckx.

References

Alpkvist E, Klapper I. 2007. Description of mechanical response including detachment using a novel particle model of biofilm/flow interaction. Water Sci Technol 55:265–273.

Besemer K, Singer G, Hödl I, Battin TJ. 2009. Bacterial community composition of stream biofilms in spatially variable-flow environments. Appl Environ Microbiol 75: 7189–7195.

Bishop PL, Gibbs JT, Cunningham BE. 1997. Relationship between concentration and hydrodynamic boundary layers over biofilms. Environ Technol 18:375–386.

Bissett A, de Beer D, Schoon R, Shiraishi F, Reimer A, Arp G. 2008. Microbial mediation of stromatolite formation in karst-water creeks. Limnol Oceanogr 53:1159–1168.

Brindle ER, Miller DA, Stewart PS. 2011. Hydrodynamic deformation and removal of *Staphylococcus epidermidis* biofilms treated with urea, chlorhexidine, iron chloride, or DispersinB. Biotechnol Bioeng 108:2968–2977.

Characklis WG, Turakhia MH, Zelver N. 1990. Transport and interfacial transfer phenomena. In: Characklis WG, Marshall KC, editors. Biofilms. New York (USA): John Wiley & Sons. p. 265–340.

Christiansen P, Hollesen L, Harremoes P. 1995. Liquid-film diffusion on reaction rate in submerged biofilters. Water Res 29:947–952.

Cogan NG. 2008. Two-fluid model of biofilm disinfection. Bull Math Biol 70:800–819.

Davison WM, Pitts B, Stewart PS. 2010. Spatial and temporal patterns of biocide action against *Staphylococcus epidermidis* biofilms. Antimicrob Agents Chemother 54: 2920–2927.

de Beer D, Stoodley P. 2006. Microbial biofilms. In: Dworkin M, Falkow S, Rosenberg E, Schleifer KH, Stackebrandt E, editors. The prokaryotes. New York (USA): Springer-Verlag. p. 904–937.

de Beer D, Stoodley P, Lewandowski Z. 1994a. Liquid flow in heterogeneous biofilms. Biotechnol Bioeng 20:636–641.

de Beer D, Stoodley P, Lewandowski Z. 1997. Measurements of local diffusion coefficients in biofilms by microinjection and confocal microscopy. Biotechnol Bioeng 53:151–158.

de Beer D, Stoodley P, Roe F, Lewandowski Z. 1994b. Effects of biofilm structure on oxygen distribution and mass transport. Biotechnol Bioeng 43:1131–1138.

Debus O, Baumgartl H, Sekoulov I. 1994. Influence of fluid velocities on the degradation of volatile aromatic-compounds in membrane-bound biofilms. Water Sci Technol 29:253–262.

Dockery J, Klapper I. 2001. Finger formation in biofilm layers. SIAM J Appl Math 62:853–869.

Dunsmore BC, Jacobsen A, Hall-Stoodley L, Bass CJ, Lappin-Scott HM, Stoodley P. 2002. The influence of fluid shear on the structure and material properties of sulphate-reducing bacterial biofilms. J Ind Microbiol Biotechnol 29:347–353.

Eberl HJ, Sudarsan R. 2008. Exposure of biofilms to slow flow fields: the convective contribution to growth and disinfection. J Theor Biol 253:788–807.

Fowler JD, Robertson CR. 1991. Hydraulic permeability of immobilized bacterial cell aggregates. Appl Environ Microbiol 57:102–113.

Fux CA, Wilson S, Stoodley P. 2004. Detachment characteristics and oxacillin resistance of *Staphyloccocus aureus* biofilm emboli in an in vitro catheter infection model. J Bacteriol 186:4486–4491.

Gantzer CJ, Rittmann BE, Herricks EE. 1988. Mass-transport to streambed biofilms. Water Res 22:709–722.

Gjersing EL, Codd SL, Seymour JD, Stewart PS. 2005. Magnetic resonance microscopy analysis of advective transport in a biofilm reactor. Biotechnol Bioeng 89:822–834.

Graba M, Moulin FY, Boulêtreau S, Garabétian F, Kettab A, Eiff O, Sánchez-Pérez JM, Sauvage S. 2010. Effect of near-bed turbulence on chronic detachment of epilithic biofilm: experimental and modeling approaches. Water Resour Res 46:W11531.

Han P, Bartels DM. 1996. Temperature dependence of oxygen diffusion in H_2O and D_2O. J Phys Chem 100:5597–5602.

Hermanowicz SW. 1999. Two dimensional simulations of biofilm development: effects of external environmental conditions. Water Sci Technol 39:107–114.

Horn H, Hempel DC. 1995. Mass transfer coefficients for an autotrophic and a heterotrophic biofilm system. Water Sci Technol 32:199–204.

Horn H, Wäsche S, Hempel DC. 2002. Simulation of biofilm growth, substrate conversion and mass transfer under different hydrodynamic conditions. Water Sci Technol 46:249–252.

Hornemann JA, Codd SL, Fell RJ, Stewart PS, Seymour JD. 2009. Secondary flow mixing due to biofilm growth in capillaries of varying dimensions. Biotechnol Bioeng 103: 353–360.

Horswill AR, Stoodley P, Stewart PS, Parsek MR. 2007. The effect of the chemical, biological, and physical environment on quorum sensing in structured microbial communities. Anal Bioanal Chem 387:371–380.

Johnson EM, Deen WM. 1996. Hydraulic permeability of agarose gels. AIChE J 42:1220–1224.

Kirisits MJ, Margolis JJ, Purevdorj-Gage BL, Vaughan B, Chopp DL, Stoodley P, Parsek MR. 2007. Influence of the hydrodynamic environment on quorum sensing in *Pseudomonas aeruginosa* biofilms. J Bacteriol 189:8357–8360.

Kühl M, Jørgensen BB. 1992. Microsensor measurements of sulfate reduction and sulfide oxidation in compact microbial communities of aerobic biofilms. Appl Environ Microbiol 58:1164–1174.

La Motta EJ. 1976. External mass transfer in a biological film reactor. Biotechnol Bioeng 28:1359–1370.

Lee JH, Kaplan JB, Lee WY. 2008. Microfluidic devices for studying growth and detachment of *Staphylococcus epidermidis* biofilms. Biomed Microdevices 10:489–498.

Lewandowski Z, Altobelli SA, Fukushima E. 1993. NMR and microelectrode studies of hydrodynamics and kinetics in biofilms. Biotechnol Prog 9:40–45.

Lewandowski Z, Altobelli SA, Majors PD, Fukushima E. 1992. NMR imaging of hydrodynamics near microbially colonized surfaces. Water Sci Technol 26:577–584.

Li SY, Chen GH. 1994. Modeling the organic removal and oxygen-consumption by biofilms in an open-channel flow. Water Sci Technol 30:53–61.

Libicki SB, Salmon PM, Robertson CR. 1988. The effective diffusive permeability of a nonreacting solute in microbial cell aggregates. Biotechnol Bioeng 32:68–85.

Manz B, Volke F, Goll D, Horn H. 2003. Measuring local flow velocities and biofilm structure in biofilm systems with magnetic resonance imaging (MRI). Biotechnol Bioeng 84:424–432.

Masic A, Bengtsson J, Christensson M. 2010. Measuring and modeling the oxygen profile in a nitrifying moving bed biofilm reactor. Math Biosci 227:1–11.

McDonogh R, Schaule G, Flemming H.-C. 1994. The permeability of biofouling layers on membranes. J Membrane Sci 87:199–217.

Nir A, Pismen LM. 1977. Simultaneous intraparticle forced convection, diffusion, and reaction in a porous catalyst. Chem Eng Sci 32:35–41.

Nishihara GN, Ackerman JD. 2007. On the determination of mass transfer in a concentration boundary layer. Limnol Oceanogr Meth 5:88–96.

Ohl AL, Horn H, Hempel DC. 2004. Behaviour of biofilm systems under varying hydrodynamic conditions. Water Sci Technol 49:345–351.

Picioreanu C, van Loosdrecht MC, Heijnen JJ. 1998. Mathematical modeling of biofilm structure with a hybrid differential-discrete cellular automaton approach. Biotechnol Bioeng 58:101–116.

Picioreanu C, van Loosdrecht MC, Heijnen JJ. 2000. A theoretical study on the effect of surface roughness on mass transport and transformation in biofilms. Biotechnol Bioeng 68:355–369.

Picioreanu C, Vrouwenvelder JS, van Loosdrecht MCM. 2009. Three-dimensional modeling of biofouling and fluid dynamics in feed spacer channels of membrane devices. J Membrane Sci 345:340–354.

Picologlou BF, Zelver N, Characklis WG. 1980. Biofilm growth and hydraulic performance. J Hyd Div ASCE 106:733–746.

Purevdorj-Gage, LB, Stoodley P. 2004. Biofilm structure, behavior, and hydrodynamics. In: Ghannoum M, O'Toole GA, editors. Microbial biofilms. Washington (DC): ASM Press. p. 160–173.

Rani SA, Pitts B, Stewart PS. 2005. Rapid diffusion of fluorescent tracers into *Staphylococcus epidermidis* biofilms visualized by time lapse microscopy. Antimicrob Agents Chemother 49:728–732.

Rasmussen K, Lewandowski Z. 1998. Microelectrode measurements of local mass transport rates in heterogeneous biofilms. Biotechnol Bioeng 59:302–309.

Roberts RD, Revsbech NP, Damgaard LR. 2007. Effect of water velocity and benthic diatom morphology on the water chemistry experienced by post-larval abalone. J Shellfish Res 26:745–750.

Rochex A, Godon JJ, Bernet N, Escudié R. 2008. Role of shear stress on composition, diversity and dynamics of biofilm bacterial communities. Water Res 42:4915–4922.

Roy H, Huttel M, Jørgensen BB. 2002. The role of small-scale sediment topography for oxygen flux across the diffusive boundary layer. Limnol Oceanogr 47:837–847.

Rupp CJ, Fux CA, Stoodley P. 2005. Viscoelasticity of *Staphylococcus aureus* biofilms in response to fluid shear allows resistance to detachment and facilitates rolling migration. Appl Environ Microbiol 71:2175–2178.

Rusconi R, Lecuyer S, Guglielmini L, Stone HA. 2010. Laminar flow around corners triggers the formation of biofilm streamers. J R Soc Interface 7:1293–1299.

Rusconi R, Lecuyer S, Autrusson N, Guglielmini L, Stone HA. 2011. Secondary flow as a mechanism for the formation of biofilm streamers. Biophys J 100:1392–1399.

Salek MM, Sattari P, Martinuzzi RJ. 2011. Analysis of fluid flow and wall shear stress patterns inside partially filled agitated culture well plates. Ann Biomed Eng [Epub ahead of print]. DOI: 10.1007/s10439-011-0444-9.

Sangani AS, Acrivos A. 1982. Slow flow through a periodic array of spheres. Int J Multiphase Flow 8:343–360.

Schultz MP, Swain GW. 1999. The effect of biofilms on turbulent boundary layers. J Fluids Eng 121:44–51.

Seymour JD, Codd SL, Gjersing EL, Stewart PS. 2004a. Magnetic resonance microscopy of biofilm structure and impact on transport in a capillary bioreactor. J Magn Reson 167:322–327.

Seymour JD, Gage JP, Codd SL, Gerlach R. 2004b. Anomalous fluid transport in porous media induced by biofilm growth. Phys Rev Lett 93: 198103-1-198103-4.

Siegrist H, Gujer W. 1987. Demonstration of mass transfer and pH effects in a nitrifying biofilm. Water Res 21:1481–1487.

Simões M, Pereira MO, Vieira MJ. 2005. Effect of mechanical stress on biofilms challenged by different chemicals. Water Res 39:5142–5152.

Simões M, Pereira MO, Vieira MJ. 2007. The role of hydrodynamic stress on the phenotypic characteristics of single and binary biofilms of *Pseudomonas fluorescens*. Water Sci Technol 55:437–445.

Simões M, Simões LC, Vieira MJ. 2008. Physiology and behavior of *Pseudomonas fluorescens* single and dual strain biofilms under diverse hydrodynamics stresses. Int J Food Microbiol 128:309–316.

Singer G, Besemer K, Hochedlinger G, Chlup AK, Battin TJ. 2011. Monomeric carbohydrate uptake and structure-function coupling in stream biofilms. Aquat Microb Ecol 62:71–83.

Staal M, Borisov SM, Rickelt LF, Klimant I, Kühl M. 2011. Ultrabright planar optodes for luminescence life-time based microscopic imaging of O_2 dynamics in biofilms. J Microbiol Meth 85:67–74.

Stewart PS. 1998. A review of experimental measurements of effective diffusive permeabilities and effective diffusion coefficients in biofilms. Biotechnol Bioeng 59: 261–272.

Stewart PS. 2003. Diffusion in biofilms. J Bacteriol 185:1485–1491.

Stewart PS, Davison WM, Steenbergen JN. 2009. Daptomycin rapidly penetrates a *Staphylococcus epidermidis* biofilm. Antimicrob Agents Chemother 53:3505–3507.

Stoodley P, de Beer D, Lewandowski Z. 1994. Liquid flow in biofilm systems. Appl Environ Microbiol 60:2711–2716.

Stoodley P, Lewandowski Z, Boyle JD, Lappin-Scott HM. 1998. Oscillation characteristics of biofilm streamers in turbulent flowing water as related to drag and pressure drop. Biotechnol Bioeng 57:536–544.

Stoodley P, Lewandowski Z, Boyle JD, Lappin-Scott HM. 1999. Structural deformation of bacterial biofilms caused by short-term fluctuations in fluid shear: An in situ investigation of biofilm rheology. Biotechnol Bioeng 65: 83–92.

Stoodley P, Yang S, Lappin-Scott H, Lewandowski Z. 1997. Relationship between mass transfer coefficient and liquid flow velocity in heterogenous biofilms using microelectrodes and confocal microscopy. Biotechnol Bioeng 56: 681–688.

Stoodley P, Cargo R, Rupp CJ, Wilson S, Klapper I. 2002. Biofilm material properties as related to shear-induced deformation and detachment phenomena. J Ind Microbiol Biotechnol 29:361–367.

Stoodley P, Dodds I, De Beer D, Scott HL, Boyle JD. 2005. Flowing biofilms as a transport mechanism for biomass through porous media under laminar and turbulent conditions in a laboratory reactor system. Biofouling 21: 161–168.

Stoodley P, Wilson S, Hall-Stoodley L, Boyle JD, Lappin-Scott HM, Costerton JW. 2001b. Growth and detachment of cell clusters from mature mixed species biofilms. Appl Environ Microbiol 67:5608–5613.

Stoodley P, Jacobsen A, Dunsmore BC, Purevdorj B, Wilson S, Lappin-Scott HM, Costerton JW. 2001a. The influence of fluid shear and $AlCl_3$ on the material properties of *Pseudomonas aeruginosa* PA01 and *Desulfovibrio* sp. EX265 biofilms. Water Sci Technol 43:113–120.

Taherzadeh D, Picioreanu C, Küttler U, Simone A, Wall WA, Horn H. 2010. Computational study of the drag and oscillatory movement of biofilm streamers in fast flows. Biotechnol Bioeng 105:600–610.

Teodósio JS, Simões M, Melo LF, Mergulhão FJ. 2011. Flow cell hydrodynamics and their effects on *E. coli* biofilm formation under different nutrient conditions and turbulent flow. Biofouling 27:1–11.

Towler BW, Cunningham AB, Stoodley P, McKittrick L. 2006. A model of fluid-biofilm interaction using a Burger material law. Biotechnol Bioeng 96:259–271.

van Dyke M. 1982. An album of fluid motion. Stanford (CA): Parabolic Press. 176 pp.

van Loosdrecht MC, Heijnen JJ, Eberl H, Kreft J, Picioreanu C. 2002. Mathematical modelling of biofilm structures. Antonie Leeuwenhoek 81:245–256.

Vaughan BL Jr, Smith BG, Chopp DL. 2010. The influence of fluid flow on modeling quorum sensing in bacterial biofilms. Bull Math Biol 72:1143–1165.

Vo GD, Heys J. 2011. Biofilm deformation in response to fluid flow in capillaries. Biotechnol Bioeng 108:1893–1899.

Vo GD, Brindle E, Heys J. 2010. An experimentally validated immersed boundary model of fluid-biofilm interaction. Water Sci Technol 61:3033–3040.

Wagner M, Manz B, Volke F, Neu TR, Horn H. 2010. Online assessment of biofilm development, sloughing and forced detachment in tube reactor by means of magnetic resonance microscopy. Biotechnol Bioeng 107:172–181.

Wäsche S, Horn H, Hempel DC. 2002. Influence of growth conditions on biofilm development and mass transfer at the bulk/biofilm interface. Water Res 36:4775–4784.

Yang S, Lewandowski Z. 1995. Measurement of local mass transfer coefficient in biofilms. Biotechnol Bioeng 48: 737–744.

Yang YX, Liao Q, Zhu X, Wang H, Wu R, Lee DJ. 2011. Lattice Boltzmann simulation of substrate flow past a cylinder with PSB biofilm for bio-hydrogen production. Intl J Hydrogen Energy 36:14031–14040.

Yu T, de la Rossa C, Lu R. 2004. Microsensor measurement of oxygen concentration in biofilms: from one dimension to three dimensions. Water Sci Technol 49:353–358.

Zhang TC, Bishop PL. 1994. Experimental determination of the dissolved oxygen boundary layer and mass transfer resistance near the fluid biofilm interface. Water Sci Technol 30:47–58.

Zhang W, Sileika TS, Chen C, Liu Y, Lee J, Packman AI. 2011. A novel planar flow cell for studies of biofilm heterogeneity and flow-biofilm interactions. Biotechnol Bioeng 108:2571–2582.

Zhu S, Chen S. 2001. Impacts of Reynolds number on nitrification biofilm kinetics. Aquacult Eng 24:213–229.